Springer

KSME

Journal of Mechanical Science and Technology 33 (9) (2019) 4421~4429
www.springerlink.com/content/1738-494x(Print)/1976-3824(Online)
DOI 10.1007/s12206-019-0838-4

Study on flexible two-axis roll-bending process for component with non-circular section †

Tao Zhang*, Huapu Sha, Shihong Lu, Chao Du and Peng Chen

College of Mechanic and Electrical Engineering, Nanjing University of Aeronautics and Astronautics, Nanjing, China

(Manuscript Received February 25, 2019; Revised May 3, 2019; Accepted May 21, 2019)

Abstract

Two-axis roll-bending technology, with the advantages of small curvature radius, short straight section and high efficiency, is widely used in fields of aerospace and automobile. By adjusting indentation depth in two-axis roll-bending process, different curvature radius of circular and elliptic component can be formed. Roll-bending experiments and numerical simulations for component with circular and elliptic section are conducted. The results show that the forming curvature radius of circular component and its deviation both decrease with ascending indentation depth. The relationship between forming curvature radius and indentation depth is polynomial fitted. On this basis, ellipse parameter equation is established and different curvature radius at different position of the ellipse is achieved by adjustment of indentation depth. The relationship between indentation depth and forming time is obtained for elliptic component. Elliptic components with different sizes are formed. The stress distribution is uniform after roll-bending process and it increases with ascending indentation depth.

Keywords: Two-axis roll-bending process; Forming curvature radius; Indentation depth; Elliptic section

1. Introduction

Roll-bending forming, especially for circular component with single curvature, is widely used in fields of aerospace, marine engineering and automobile. With the development of aerospace industry, requirements of components with non-circular section and variable curvature are gradually increased, such as leading edge skin and auto exhaust pipe of the airplane. The commonly used methods for this kind of components are described as follows: Firstly, component with circular section is formed by roll-bending process and then it is turned into non-circular section by die pressing. High cost and long production cycle are the main disadvantages of this method. In addition, three-roll bending and four-roll bending process can be used to form components with variable curvature. However, the distance between thelower rolls has to be changed for different curvature radius during roll-bending process. The low efficiency, complex operation and low forming precision affect the application of three-roll bending and four-roll bending process. Compared to the method mentioned above, two-axis roll-bending technology is beneficial to improve forming accuracy and efficiency as well as forming quality. Furthermore, the variable curvature radius is achieved as long as the indentation depth is changed, which can be imported into the control system before roll-bending process. The schematic diagram of two-axis roll-bending process is shown in Fig. 1. Two-axis flexible roll-bending machineconsists of rigid roll, flexible roll (the central spindle is covered by polyurethane rubber) and accurate press fit servo system. The flexible roll is drive roll and it rotates at a low speed. A loading force P is applied to rigid roll and a indentation depth f is generated. The bending deformation of the plate is generated through the distributed pressure formed by the rigid roll and elastic layer of the flexible roll. A forming curvature radius r of the plate is obtained after the roll-bending process. Therefore, different forming curvature radius can be achieved by different indentation depth resulting from variation of loading force.

Many previous studies had been conducted on roll-bending process, including analytical models, finite element models (FEM) and experimental investigations. Plettke and Vatter [1] presented two new approaches to simulate the bending radius during the three-roll-push-bending process. The first one was based on analytically derived moment-curvature relationship which considered the realistic flow behavior; while the second one was using beam elements. Fu et al. [2] proposed an analytical model and FEM for investigating the three-roll bending forming process, and accurate relationship between the downward inner roller displacement and the desired springback radius (unloaded curvature radius) of the bent plate was obtained.

*Corresponding author. Tel.: +86 15250997258, Fax.: +86 2584892585
E-mail address: 297zhangtao@nuaa.edu.cn
† Recommended by Associate Editor Yongho Jeon
© KSME & Springer 2019

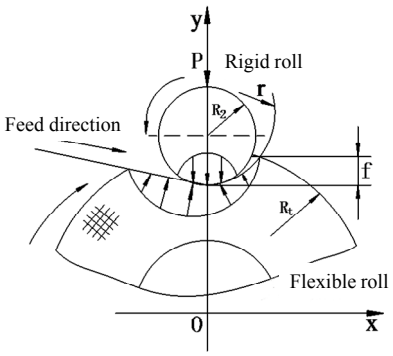

Fig. 1. Schematic diagram of two-axis roll-bending process.

Salem et al. [3] developed an analytical model to study the effects of material properties and process parameters (plate thickness, yield stress, curvature, and conicity for a truncated cone) on roll bending force, residual stresses, and power of roll bending process. Tran et al. [4] developed a 3D dynamic FEM model of an asymmetrical roll bending process and investigated the effects of parameters on the final shape accuracy, the bending forces, and the residual strains. Chudasama and Raval [5] established a prediction model for the bending force of dynamic roll-bending and analyzed the spring-back of the work-piece during 3-roller conical bending process. Byon et al. [6] proposed an approximate model to predict the spread and surface profile of cross sections of material in a 3-roll rolling process. The spread at the exit of roll gap was the function of the roll diameter, area fraction of the cross section and contact length of the roll and material. Asymmetrical three-roll bending was widely used in metal forming due to its simple configuration. Feng and Champliaud [7] studied the prediction of the position of the lateral roll with a bilinear material model during cylindrical roll bending. Tajyar and Masoumi [8] investigated the effect of shape rolling process on the bond strength and mechanical properties of Al/Cu bimetal pipesand found that with the increase of roll gap reduction during the various stages, the hardness increased, while the shear strength decreased. Leacock et al. [9] presented a FEM methodology of four roll bending process and it was validated by comparison with force and curvature measurements from the machine. Gandhi et al. [10] discussed the formulation of spring-back and machine setting parameters for continuous multi-pass bending of cone frustum on three-roller bending machines with non-compatible (cylindrical) rollers, and then analyzed the effect of change of flexural modulus on spring-back prediction. Cai et al. [11] studied a new flexible forming technology of roll bending: An upper flexible roll and two lower flexible rolls as a forming tool, in which the shape of a flexible roll could be changed in vertical direction. Zhu et al. [12] concluded that the commonly used material constitutive model predicted the spring-back of cold-bending poorly and established a new constitutive model considering the elastic behavior, the anisotropy, and the work-hardening. Shim et al. [13] proposed two different approaches to avoid a wavy edge for a formed panel, which was the main defect that appeared in corrugated panels subjected to high amounts of bending deformation, and found that the two proposed design strategies could minimize wavy edges through experimental and numerical results. Sui et al. [14] established the longitudinal and transverse mathematical models to predict the curvatures in roll bending process and the models were verified by comparisons of the desired and the numerical simulation results. Sedighi et al. [15] studied the residual stresses distribution in thin sheets of bi-layer Al-Cu sheet during roll bending process through hole-drilling method and obtained the basic formulations of converting experimentally measured strains into residual stress. Wang et al. [16] analyzed the forming precision of flexible rolling and the reasons for the shape errors through simulated and experimental results, which demonstrated that the proposed process was a feasible and effective way of forming three-dimensional surface parts. Jiao et al. [17] developed an analytical solution for the prediction of web-warping that considers both geometric and material parameters as web-warping defect is the major problem in flexible roll forming. Continuous flexible roll forming is an effective sheet metal-forming process used to manufacture three-dimensional surface parts. Cai et al. [18] established a system of methods for controlling the continuous forming process and presented the formulations to determine the downward displacement of upper roll. As a result, the software for controlling continuous flexible roll forming process was developed. Wang et al. [19] introduced the improvement of the continuous-forming process that the curve radius of the roll gap was much larger than the transverse curvature radius of the forming surface in the forming process. Three-dimensional deformation was generated due to the residual stress caused by the longitudinal non-uniform elongation. Cai et al. [20] set forth the mechanism of the three-dimensional surface formation in continuous roll forming and presented the governing equations for the bending deformation in rolling process, then derived the formulation to calculate the longitudinal bending deformation. The in-plane roll-bending of strip (IRS) is a flexible forming process to produce ring parts and instability modes (including external wrinkling, internal wrinkling) may appear under inappropriate deformation. Liu et al. [21] proposed a new hybrid method to accurately predict all these instability modes in IRS. In order to solve the axial wrinkles, poor strength and cross-section distortion of pipes with rectangular cross-sections under roll bending process, double-stage forming was applied by Shim et al. [22] and the cross-section distortion could be minimized by regulating the pre-bending radius at the first pre-bending stage. The forming forces during roll-bending process can be reduced by heating the workpieces and heat-assisted roll-bending was a promising alternative for manufacturing large and thick axisymmetric parts. Quan et al. [23] established numerical simulations of heat-assisted roll-bending to study the relationships between temperature, applied forces and plate thickness. A better understanding of the

mechanism of the process and the design of an efficient heating system to control the heat energy was achieved.

However, many previous studies were focused on bending deformation, residual stress and springback of plate during three-roll or four-roll bending process. The studies of two-axis flexible roll-bending forming were rarely published. In addition, many researchers paid much attention to the roll-bending process of components with circular section. Nevertheless, many components with non-circular section were in great need in fields of aerospace and the forming technology of this kind of component was rarely analyzed. In this study, tensile tests are conducted to obtain material parameters of aluminum alloy 2024-T351. Then, roll-bending experiments for component with circular section are performed to acquire the relationship between forming curvature radius and indentation depth. In addition, component with elliptical section is experimentally studied and different sizes and forming curvature radius can be achieved by adjustment of indentation depth. Finally, numerical models of roll-bending process are established and the stress variation at different indentation depth is analyzed. This study provides guidance two-axis roll-bending process of components with non-circular section.

2. Experiments

The experiments conducted in this study include three parts: Tensile test, roll-bending process for plate with circular section and for plate with non-circular section (such as elliptic section). Mechanical property parameters of the material, such as Young's modulus, Poisson's ratio and yield strength, can be obtained through tensile test. The material of the plate is aluminum alloy 2024-T351 and its thickness is 1 mm. According to metal tensile test standard described in GB228-87, tensile test of aluminum alloy 2024-T351 is conducted on tensile testing machine. The gauge length is 50mm and width of tensile area is 12.5 mm. The loading speed of tensile testing machine is 0.05 mm/s and its static load error is less than 0.1 %. Laser extensometer is used to calculate the elongation of the specimen after tensile test and its gauge length is 50 mm. During the tensile test, the load, displacement, strain and time are recorded automatically. The stress-strain curve of the material can be obtained.

Two-axis flexible roll-bending machine is used for the roll-bending process of metal alloy, such as aluminum alloy, carbon steel and stainless steel, as shown in Fig. 2. The material of the flexible roll is polyurethane rubber; its thickness is 50 mm and its Shore Hardness is 90 A. The flexible roll is drive roll with diameter of 280 mm and its rotational speed is 1.2 RPM. The rigid roll is driven roll and its diameter is 80 mm.

Under the given roll diameter and plate size, the forming curvature radius of the plate is related to indentation depth during roll-bending process. Roll-bending experiments for component with circular section are conducted to obtain the relationship between forming curvature radius and indentation depth. The size of the plate is 400 mm (length) ×100 mm (width) ×1 mm (thickness) and the indentation depth in roll-bending process varies from 3 mm to 5.5 mm. As the component with noncircular section can be divided into many arcs and each arc can be assumed to part of circle under large number of arcs. Therefore, the roll-bending process for non-circular section can be achieved on the basis of the results from circular section. After that, roll-bending experiments for component with noncircular section (such as elliptic section) are conducted. After roll-bending experiments, several points on the surface of the component are measured by coordinate measuring machine and forming curvature radius can be obtained.

Table 1. Results of tensile test of aluminum alloy 2024-T351.

Specimen NO.	*E*/GPa	σ_s/*MPa*	*K*/*MPa*	*n*	σ_b/*MPa*
1	72.01	319.46	456.03	0.21	413.16
2	72.16	321.55	468.65	0.24	416.23
3	71.88	322.09	460.09	0.23	415.37
Average value	72.02	321.03	461.03	0.23	414.92

where σ_b is ultimate strength.

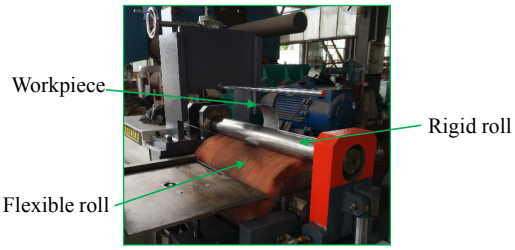

Fig. 2. Two-axis flexible roll-bending machine.

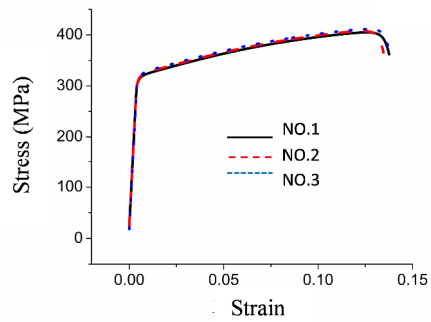

Fig. 3. True stress-strain curves during tensile test.

3. Results and discussion

3.1 Tensile test

Fig. 3 shows the true stress-strain curves of aluminum alloy 2024-T351 and there are obvious elsticity stage and plasticity stage in the tensile test. The stress first increases linearly with strain and then increases nonlinearly. Piecewise function can

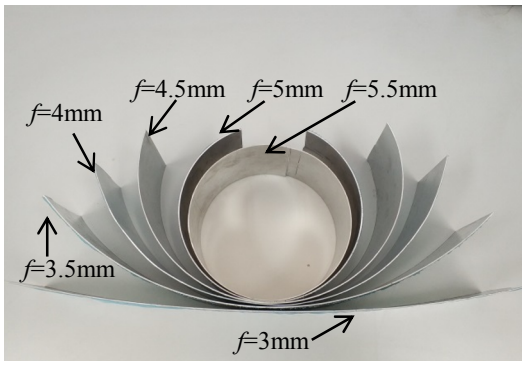

Fig. 4. Roll-bending components for different indentation depths.

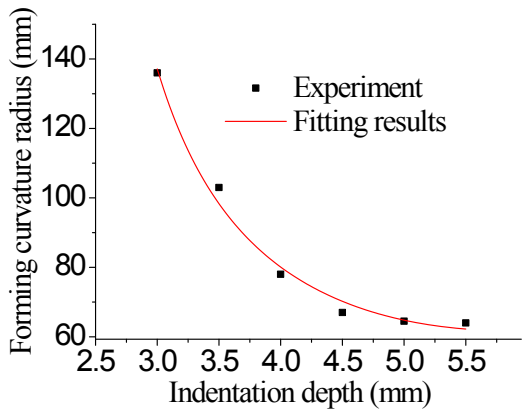

Fig. 5. Effect of indentation depth on forming curvature radius.

be used to describe deformation behavior during tensile test, as shown in Eq. (1). The results of material parameters are shown in Table 1.

$$\sigma=\begin{cases} E\varepsilon_e & \varepsilon \le \sigma_s / E \\ \sigma_s + K(\varepsilon-\varepsilon_e)^n & \varepsilon > \sigma_s / E \end{cases} \quad (1)$$

where E is Young's modulus, ε is strain and ε_e is elastic strain, σ_s is yield strength, K and n are hardening coefficient and exponent, respectively.

3.2 Roll-bending for component with circular section

For the two-axis roll-bending process, the forming curvature radius is related to indentation depth under given roll diameters. Different indentation depths are adopted in the roll-bending process for component with circular section, the figures of the components after roll-bending are shown in Fig. 4. After measuring position of the points at surface of the component, the forming curvature radius is fitted, as shown in Fig. 5. The forming curvature radius first decreases sharply and then decreases slightly with ascending indentation depth. When the indentation depth exceeds 4.5 mm, the forming curvature radius almost keeps steady, which illustrates further increase of indentation depth has little effect on curvature radius decrease. The forming force between flexible roll and rigid roll is quite small under small indentation depth, as a result, small bending curvature is generated due to small bending moment. The forming force and bending moment both increase with ascending indentation depth. The relationship between forming curvature radius and indentation depth can be obtained by quadratic fitting, as shown in Eq. (2). In order to study the bending quality variation, deviation of the forming curvature radius is analyzed, as shown in Fig. 6. For the given indentation depth, several specimens are formed and the deviation of the forming curvature radius of these specimens is calculated. It is obvious that the deviation decreases with ascending indentation depth. Fig. 6 shows linear relationship between deviation and indentation depth up to a indentation depth of 4.5, thereafter it continues to decrease with a different ratio, piecewise linear function is adopted to describe the relationship between deviation of forming curvature radius and indentation depth, as shown in Eq. (3). The bending moment applied to the plate from polyurethane rubber is quite small under small indentation depth, which cannot meet stability requirements of roll-bending process. In addition, the forming curvature radius changes sharply under small indentation depth, the variation of indentation depth can cause large fluctuation of forming curvature radius. Therefore, the deviation of indentation depth adjustment under small indentation depth may induce large deviation of forming curvature radius.

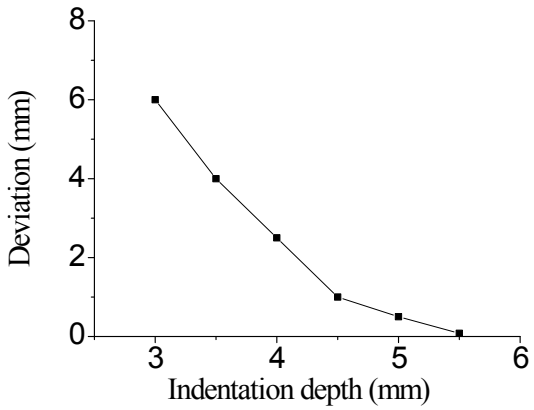

Fig. 6. Effect of indentation depth on deviation of forming curvature radius.

$$r = 1/(-0.02176 + 0.01305 f - 0.00112 f^2) \quad (2)$$

where r is forming curvature radius and f is indentation depth.

$$D_e=\begin{cases} -3.33r + 15.99 & r \le 4.5 \\ -0.92r + 5.14 & r > 4.5 \end{cases} \quad (3)$$

where D_e is deviation of forming curvature radius.

3.3 Roll-bending for component with elliptic section

Component with non-circular section is commonly seen in

Table 2. Parameters of specimen with elliptic section.

Specimen number	a (mm)	b (mm)	r_{min} (mm)	r_{max} (mm)
1	90	80	71.1	101.2
2	100	80	64	125
3	100	90	81	111.1
4	110	90	73.6	134.4

the field of aerospace, such as the skin at leading edge of the wing. Elliptic section is a typical type of non-circular section as its curvature obviously changes at different positions. Firstly, ellipse parameter equation is established and the curvature radius at different positions of the ellipse is calculated, as shown in Eqs. (4) and (5), the value range of curvature radius is $b^2/a \le r \le a^2/b$.

$$\begin{cases} x = a\cos\theta \\ y = b\sin\theta \end{cases} \tag{4}$$

$$r = \left| \frac{\left(1+\left(\frac{b\sin\theta}{a\cos\theta}\right)\right)^{1.5}}{\frac{b}{a^2\left(\sin\theta\right)^3}} \right| \tag{5}$$

where a is semi-major axis and b is semi-minor axis, θ is angle with horizontal axis.

In this study, four specimens with elliptic section are studied and different size of ellipse is shown in Table 2. As discussed above, different curvature radius is achieved by adjustment of indentation depth during roll-bending process. The curvature radius changes with the point's position of the ellipse and the indentation depth is adjusted according to the arc length and the forming time. The forming time t can be calculated by the arc length and the velocity of flexible roll, as shown in Eq. (6).

$$L = a\int_0^{2\pi} \sqrt{1-\mathrm{e}^2\cos^2(\theta)}\,d\theta \tag{6}$$

where L is arc length and e is eccentricity and e is calculated by $\mathrm{e} = \sqrt{a^2-b^2}\,/\,a$.

However, the arc length is quite difficult to be calculated by Eq. (6), numerical integration is adopted. The ellipse perimeter is divided into several arcs according to the angle θ. Each arc is assumed with single curvature and the indentation depth can be set as a constant value. The accuracy of this assumption can be guaranteed as long as more arcs are divided. Compound Simpson formula is used to calculate each arc, as shown in Eq. (7).

According to Simpson equation, the integration of the specified function can be obtained by calculation of the area between the quadratic parabola and horizontal axis. It should be noted that this quadratic parabola must pass through three given points, which divided the integrating range into two parts. In order to improve the accuracy of numerial integration, compound Simpson equation is described as follows: First, the integrating range of Eq. (5) is divided into several smaller integrating range, and then Simpson equation is used in every small Simpson equation; finally, the sum of all the Simpson equation is calculated.

$$L_n = \frac{h}{6}\sum_k^{n-1}\left(S(\theta_k) + 4S\left(\theta_{k+\frac{1}{2}}\right) + S(\theta_{k+1}) \right) \tag{7}$$

where n is the number of arc, h is integration step, $h = \theta_{k+1}-\theta_k$, $S(\theta_k)$ is the value of integrand of arc length at θ_k, $S(\theta_k) = a\sqrt{1-e^2\cos^2(\theta_k)}$.

Table 3. Parameters of elliptic section (a = 100 mm, b = 80 mm) during roll-bending process.

θ(°)	r(mm)	f(mm)	L(mm)	t(s)
0~5	64	5.17	7.65	0.31
5~15	65.64	4.92	15.51	0.69
15~25	70.42	4.46	15.84	0.70
25~35	77.96	4.04	16.16	0.72
35~45	87.56	3.72	16.43	0.73
45~55	98.17	3.49	16.63	0.74
55~65	108.51	3.32	16.71	0.75
65~75	117.19	3.20	16.67	0.74
75~85	122.97	3.14	16.52	0.74
85~90	125	3.11	8.17	0.33

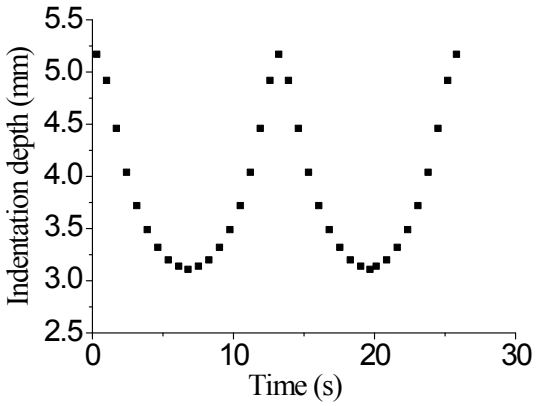

Fig. 7. Relationship between indentation depth and time for elliptic section roll-bending.

Take the component with elliptic section for example, Table 3 shows the parameters of elliptic section (a = 100 mm, b = 80 mm). The curvature radius in each arc is different and it can be achieved by different indentation depth. Fig. 7 shows the relationship between indentation depth and time during roll-bending for component with elliptic section. The data is imported into the control system by writing machining code. As the indentation depth is the main factor for the accuracy of the experiment, the starting point should be accurately posi-

Table 4. Size of test specimens after roll-bending.

Specimen number	a (mm)	b (mm)
1	88.93	80.75
2	98.12	81.25
3	98.74	91.28
4	107.56	92.16

Fig. 8. Test specimens with elliptic section after roll-bending.

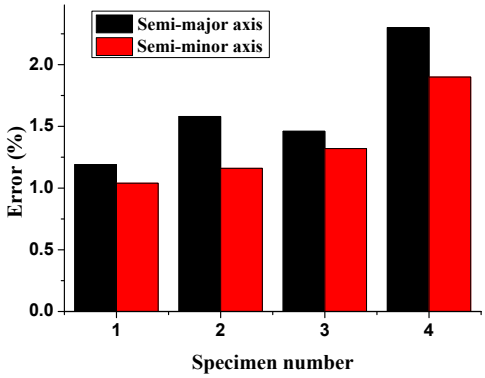

Fig. 9. Size error of elliptic specimens after roll-bending.

tioned before roll-bending process.

The test specimens with elliptic section after roll-bending are depicted in Fig. 8. After measurement of point's position by coordinate measuring machine and fitting by least square method, the sizes of semi-major axis and semi-minor axis can be calculated, as shown in Table 4. It is obviously that there are size difference between test specimens and original ones, as shown in Fig. 9. The accuracy of test specimens with elliptic section for roll-bending process is high as the maximum error is smaller than 2.5 %. Meanwhile, the error of specimen number 2 and 4 is larger than that of number 1 and 3. As shown in Table 2, the maximum curvature radius of number 2 and 4 is larger than that of number 1 and 3. Large curvature radius corresponds to small indentation depth; however, small indentation depth will increase the deviation, as discussed in Fig. 6.

Table 5. Friction coefficient for roll-bending model.

Contact bodies	Plate-rigid roll	Plate-flexible roll	Rigid roll-flexible roll
Drive	Rigid roll	Flexible roll	Rigid roll
Driven	Plate	Plate	Flexible roll
μ	0.2	0.25	0.1

4. Numerical models

There are two processes for two-axis roll-bending process: Bending forming and springback. dynamic display algorithm is used to calculate the bending curvature and stress during roll-bending process and static implicit algorithm is adopted to calculate the springback after roll-bending process.

The simulation of roll-bending process is conducted with ABAQUS software. The diameters of rigid roll and flexible roll as well as the size of the plate in numerical models are the same to experiments. The size of the plate is 400 mm (length) ×100 mm (width) ×1 mm (thickness), the thickness is much smaller than the length and width. For roll-bending process of small thickness plate, the stress variation through thickess can be neglected therefore, shell element of S4R is adopted. Three-dimensional solid element C3D8R is used for the polyurethane rubber. As there is direct contact between the plate and polyurethane rubber, the mesh size of the outer layer of polyurethane rubber is much smaller than the inner layer, as shown in Fig. 1. The mesh size of the outer layer of polyurethane rubber is nearly equal to the mesh size of the plate, high computation efficiency can be achieved on condition that the calculation precision is ensured. Elastoplastic hardening model is used to describe the relationship between true stress and true strain of aluminum alloy 2024-T351, as shown in Eq. (1). The true stress-strain curves are imported to the model to describe the variations of stress and strain during roll-bending process. The flexible roll consists of central spindle and the surrounding polyurethane rubber layer. The diameter and width of central spindle is 180 mm and 130 mm, respectively, and 280 mm and 120mm for the polyurethane rubber layer. There is no relative slip between central spindle and polyurethane rubber layer as interference fit is applied. In this model, constraint is applied between the external surface of central spindle and internal surface of polyurethane rubber layer. There are contact force and friction between rigid roll, plate and flexible roll and coulomb friction is used, as shown in Eq. (8). The friction coefficient between the three bodies is shown in Table 5.

$$f_t = p\mu \tag{8}$$

where f_t is friction force, p is normal pressure, μ is friction coefficient.

According to the indentation depth, a vertical displacement is applied to the flexible roll to simulate the loading process of flexible roll. Then rotational speed is applied to the rigid roll and flexible roll is set as driven roll to simulate the roll-

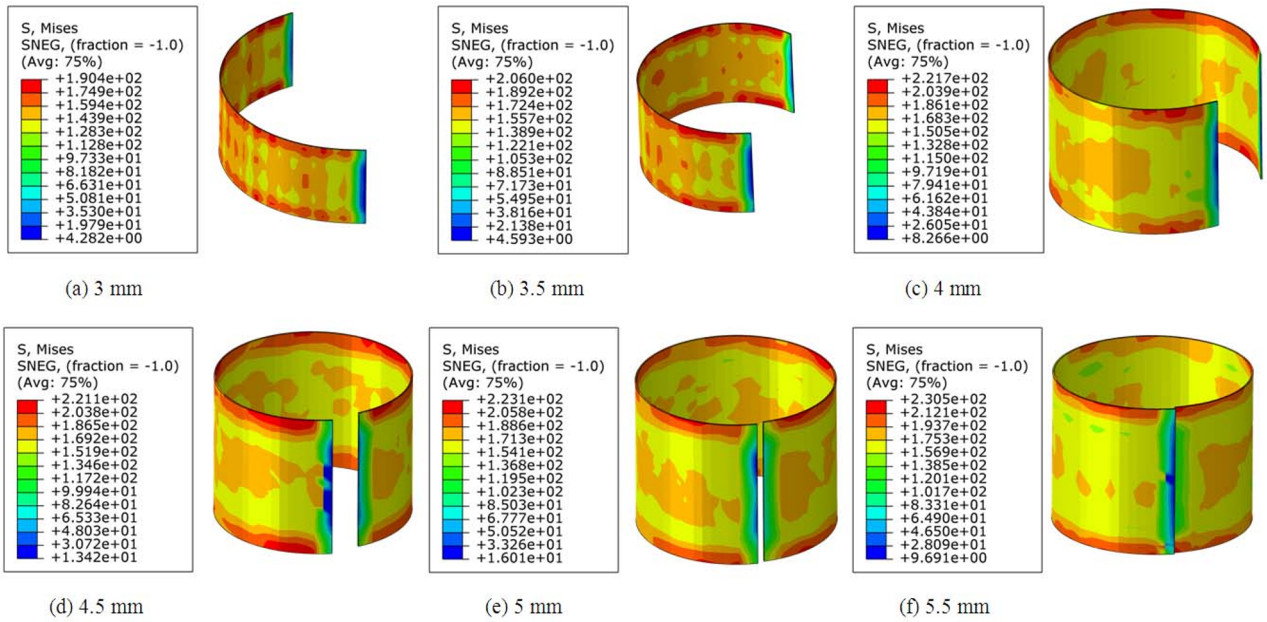

Fig. 10. Stress and forming curvature variations under different indentation depths after roll-bending process.

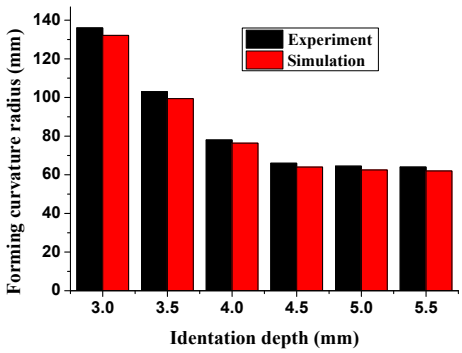

Fig. 11. Comparison of experimentlal and simulated forming curvature variations for components with circular section.

bending process. After the roll-bending process, six degrees of freedom for the short edge of the plate are constrained and the springback of the plate is analyzed. Fig. 10 shows stress and forming curvature variations under different indentation depths after roll-bending process. The maximum stress during roll-bending process increases with ascending indentation depth and the maximum stress mainly appears at both sides of the width of the plate. The stress at most area of the plate is uniform after unloading and springback process. Roll-bening is the continuous deformation process with accumulation of local small deformation, meanwhile, the width of the rolls are much larger than the plate width. The contact deformation area of the plate is completely located between two rolls. As discussed in Fig. 1, the uniform distributed pressure is applied to the plate from the flexible roll when the loading force or the indentation depth is generated. Due to the characteristics of polyurethane rubber of the flexible roll, the uniform deformation at different positions of the plate can be generated under

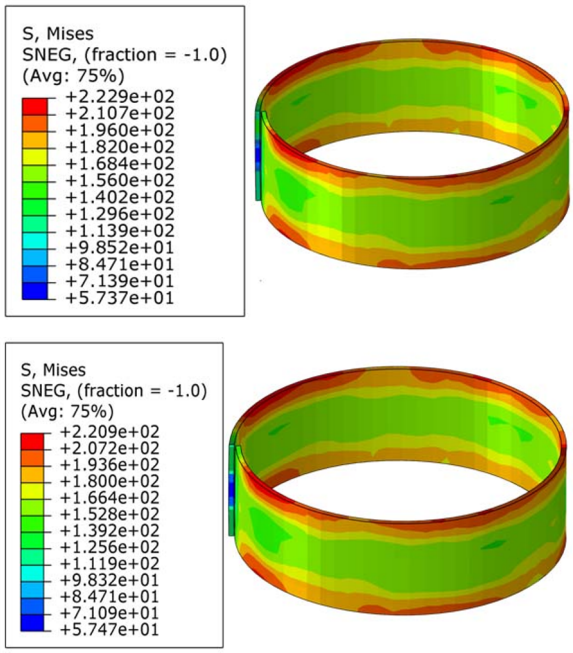

Fig. 12. Stress and forming curvature variations for components with elliptic section after roll-bending process.

the uniform pressure, as a result, the stress and strain are both small and uniformly distributed during roll-bending process. The stress at both sides of the plate is large due to no constraint along the width direction of the plate. After output of the coordiates of the nodes through the lengthwise direction of the plate, the forming curvature radius can be calculated by least square fitting method in MATLAB software. The comparison of experimentlal and simulated forming curvature

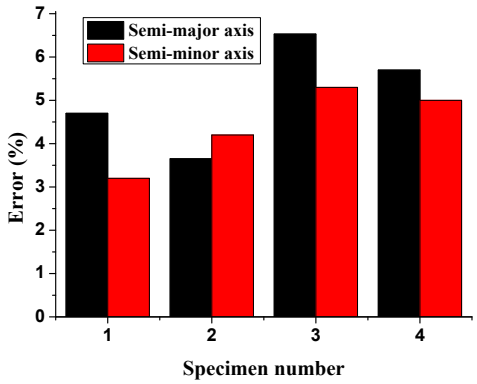

Fig. 13. Comparison of experimentlal and simulated forming curvature variations for components with elliptic section.

variations is shown in Fig. 11. The experimental results agree with the simulated results and the error ranges from 3 % to 5 %.

The simulation of roll-bending process for component with elliptic section is the same as the experiment. First, the elliptic section is divided into several arcs and then different indentation depth is applied. The results are shown in Figs. 12 and 13. The stress distribution is similar to that of circular section and the error changes from 3 % to 7 %.

5. Conclusions

(1) Numerical models of two-axis roll-bending are established and the stress after unloading increases with ascending indentation depth.

(2) The forming curvature radius decreases with ascending indentation depth and the relationship between curvature radius and indentation depth can be fitted by quadratic function for components with circular section.

(3) Through real-time adjustment of indentation depth, different curvature radius can be achieved during different time of roll-bending process.

Acknowledgments

This work was supported by the the financial support by National Natural Science Foundation of China (No. 5170 5248), Science and technology planning project of Jiangsu Province (No. BE2016179), Natural Science Foundation of Jiangsu pvovince, China (No. BK20170785) and Open Research Fund of State Key Laboratory for High Performance Complex Manufacturing, Central South University (Kfkt2017-08).

References

[1] R. Plettke and P. Vatter, Comparison of new analytical and numerical approaches to model the three-roll-push-bending process, *International Journal of Mechatronics and Manufacturing Systems,* 7 (2014) 279-295.

[2] Z. Fu, X. Tian, W. Chen, B. Hu and X. Yao, Analytical modeling and numerical simulation for three-roll bending forming of sheet metal, *International Journal of Advanced Manufacturing Technology,* 69 (2013) 1639-1647.

[3] J. Salem, H. Champliaud, Z. Feng and T. M. Dao, Experimental analysis of an asymmetrical three-roll bending process, *International Journal of Advanced Manufacturing Technology,* 83 (2016) 1823-1833.

[4] Q. H. Tran, H. Champliaud, Z. Feng and T. M. Dao, Analysis of the asymmetrical roll bending process through dynamic FE simulations and experimental study, *International Journal of Advanced Manufacturing Technology,* 75 (2014) 1233-1244.

[5] M. K. Chudasama and H. K. Raval, Bending force prediction for dynamic roll-bending during 3-roller conical bending process, *Journal of Manufaturing Processes,* 16 (2014) 284-295.

[6] S. M. Byon, S. R. Kim, T. Y. Kim and Y. Lee, An approximate model to predict the surface profile of material sections in a 3-roll rolling process, *Journal of Mechanical Science and Technology*, 31 (2017) 3489-3497.

[7] Z. Feng and H. Champliaud, Modeling and simulation of asymmetrical three-roll bending process, *Simulation Modelling Practice & Theory*, 19 (2011) 1913-1917.

[8] A. Tajyar and A. Masoumi, Investigation of mechanical properties of bimetallic square tubes produced by shape rolling of Al/Cu circular pipes, *Journal of Mechanical Science and Technology*, 30 (2016) 4299-4306.

[9] A. G. Leacock, D. McCracken, D. Brown and R. McMurray, Numerical simulation of the four roll bending process, *Materials and Manufacturing Processes,* 27 (2012) 370-376.

[10] A. H. Gandhi, A. A. Shaikh and H. K. Raval, Formulation of spring-back and machine setting parameters for multi-pass three-roller cone frustum bending with change of flexural modulus, *International Journal of Material Forming,* 2 (2009) 45-57.

[11] Z. Y. Cai, M. Z. Li and Y. W. Lan, Three-dimensional sheet metal continuous forming process based on flexible roll bending: Principle and experiments, *Journal of Materials Processing Technology,* 212 (2012) 120-127.

[12] Y. X. Zhu, Y. L. Liu, H. Yang and H. P. Li, Development and application of the material constitutive model in spring-back prediction of cold-bending, *Materials & Design,* 42 (2012) 245-258.

[13] D. S. Shim, J. Y. Son, E. M. Lee and G. Y. Baek, Improvement strategy for edge waviness in roll bending process of corrugated sheet metals, *International Journal of Material Forming,* 10 (2017) 581-596.

[14] Z. Sui, Z. Cai, Y. Lan and L. Liu, Simulation and software design of continuous flexible roll bending process for three dimensional surface parts, *Materials & Design,* 54 (2014) 498-506.

[15] M. Sedighi, J. Joudaki and H. Kheder, Residual stresses due to roll bending of bi-layer Al-Cu sheet: Experimental and analytical investigations, *The Journal of Strain Analysis*

for Engineering Design, 52 (2017) 102-111.

[16] D. Wang, M. Z. Li and Z. Cai, Research on forming precision of flexible rolling method for three-dimensional surface parts through simulation, *International Journal of Advanced Manufacturing Technology,* 71 (2014) 1717-1727.

[17] J. Jiao, B. Rolfe, J. Mendiguren and M. Weiss, An analytical model for web-warping in variable width flexible roll forming, *International Journal of Advanced Manufacturing Technology,* 86 (2016) 1541-1555.

[18] Z. Y. Cai, S. Zhou, F. X. Cai and L. Liu, Continuous flexible roll forming for three-dimensional surface part and the forming process control, *The International Journal of Advanced Manufacturing Technology,* 66 (2013) 393-400.

[19] D. Wang, M. Li and Z. Cai, Continuous-forming method for three-dimensional surface parts combining rolling process with multipoint-forming technology, *The International Journal of Advanced Manufacturing Technology,* 72 (2014) 201-207.

[20] Z. Y. Cai and M. Z. Li, Principle and theoretical analysis of continuous roll forming for three-dimensional surface parts, *Science China Technological Sciences,* 56 (2013) 351-358.

[21] N. Liu, H. Yang, H. Li and Z. J. Li, A hybrid method for accurate prediction of multiple instability modes in in-plane roll-bending of strip, *Journal of Materials Processing Technology,* 214 (2014) 1173-1189.

[22] D. S. Shim, K. P. Kim and K. Y. Lee, Double-stage forming using critical pre-bending radius in roll bending of pipe with rectangular cross-section, *Journal of Materials Processing Technology,* 236 (2016) 189-203.

[23] T. H. Quan, H. Champliaud, Z. Feng, J. Salem and T. Y. Dao, Heat-assisted roll-bending process dynamic simulation, *International Journal of Modelling and Simulation*, 33 (2013) 54-62.

Tao Zhang is a Lecturer in College of Mechanic and Electrical Engineering, Nanjing University of Aeronautics and Astronautics. He received his Doctor's degree in Mechanical Engineering from Central South University. His current research interests are metal forming, modeling of forming process and microstructure evolution, additive manufacturing process.